Atomic structure of Ag(111) saturated with chlorine: Formation of Ag_3Cl_7 clusters

B. V. Andryushechkin,[1,*] V. V. Cherkez,[1,2] E. V. Gladchenko,[1,3] G. M. Zhidomirov,[1] B. Kierren,[2] Y. Fagot-Revurat,[2] D. Malterre,[2] and K. N. Eltsov[1,3]

[1]*International Joint Laboratory IMTAS, A. M. Prokhorov General Physics Institute, Russian Academy of Sciences, Vavilov street 38, 119991 Moscow, Russia*

[2]*International Joint Laboratory IMTAS, Institut Jean Lamour - UMR CNRS 7198 - équipe 102, Departement Physique de la Matière et des Matériaux, B.P 239 - Université H. Poincaré - Nancy, F-54506 Vandoeuvre les Nancy, France*

[3]*Moscow Institute of Physics and Technology, Institutskii pereulok 9, 141700 Dolgoprudny, Moscow Region, Russia*

(Received 6 May 2011; published 10 August 2011)

The structure of saturated chlorine layer on Ag(111) has been studied with low temperature scanning tunneling microscopy and density functional theory. For the first time atomic-resolution STM images of saturated chlorine coverage have been obtained. STM images demonstrate coexistence of the domain with (3×3)-like reconstruction and numerous bright objects identified as Ag_3Cl_7 clusters. According to our model supported by DFT calculations, clusters are formed on the boundaries between the adjacent (3×3) antiphase domains. These boundaries have a characteristic triangular shape and are formed by six chlorine atoms chemisorbed on the triangular silver island with local periodicity (1×1).

DOI: 10.1103/PhysRevB.84.075452 PACS number(s): 68.43.Fg, 68.43.Bc, 68.47.Fg, 68.55.ag

I. INTRODUCTION

Interaction of chlorine with (111) plane of silver has been a subject of numerous experimental and theoretical investigations since the 1970s. The interest to this system was initiated by the important promotional role of chlorine in the industrial reaction of ethylene epoxidation.[1]

According to a number of investigations,[2–4] there are two stages of chlorine reaction with silver surfaces. On the first step, chlorine forms a chemisorbed layer, while formation of a new chemical compound (silver chloride) takes place after the completion of the chemisorbed layer. These two stages were distinguished by the peaks in the thermodesorption (TD) spectra and the chemical shift of Auger lines.[2–4] However, the exact definition of the term "saturated monolayer" appears to be not so simple. Usually a monolayer of chlorine is considered to be complete when the speed of adsorption measured at room temperature by AES/XPS drastically decreases. In principle, such a definition makes sense, since at room temperature the rate of the AgCl formation is extremely low, and, moreover, its growth occurs in the 3D mode.[2–5] As a result, the AES/XPS signal remains at the same *saturation* level up to huge chlorine doses.

However, the direct assignment of the saturation level to monolayer of chemisorbed chlorine on Ag(111) appears to be problematic. Indeed, in TD spectra of Cl/Ag(111) system a multilayer low-temperature peak appears early than a saturation of the monolayer peak occurs. As a result, the TD spectrum of saturated monolayer coverage contains both monolayer and multilayer peaks. In other words, two different chemical states should coexist on a surface at the saturation point.

First, structural studies of the chlorinated silver (111) surface performed at room temperature with LEED,[2,6–10] RT-STM,[12] and SEXAFS[11] appear to be not informative. Authors reported formation of a diffused $(\sqrt{3} \times \sqrt{3})$R30° pattern at initial stage of adsorption,[2,6,8] assigned to a vacancy honeycomb structure in a SEXAFS study by Lamble *et al.*[11] At coverage close to the saturation level the appearance of the complex LEED pattern was reported. All the published LEED patterns seem to be very similar, but interpreted in a different way. In particular, Rovida *et al.* found a distorted (3×3),[6,7] Goddard *et al.* (10×10),[8] while other authors assigned the structure to the double diffraction from epitaxial AgCl layer.[2,9] In the room temperature STM study by Andryushechkin *et al.*[12] the (17×17) periodicity was found for the saturated layer.

In the most detailed room-temperature LEED work by Bowker and Waugh[2] two diffraction patterns were observed at coverage close to saturation. One of them (pattern C) contains fractional order beams at 0.28 and 0.72 reciprocal substrate lattice units. At further increase of chlorine coverage pattern C gradually transferred to more simple pattern D, with fractional order beams remaining only at 0.72 reciprocal lattice units. Note, that pattern D was also observed by Wu *et al.*[10] for a saturated chlorine coverage.

Thus, structural studies performed at room temperature did not result in adequate models of atomic structures formed by chlorine on Ag(111). The main problem was in the lack of the coverage calibration point and the ambiguity of the chlorine amount in each of surface structures that corresponded to different LEED patterns. For many cases of halogen adsorption on (111) planes of fcc metals,[13,14] the formation of a simple $(\sqrt{3} \times \sqrt{3})$R30° structure at 1/3 ML was usually used as such a calibration point. However, the situation changed after publication of the low temperature LEED data by Shard *et al.*[15] They found out that a cooling of the Cl/Ag(111) system below 190 K leads to the *normal* behavior of a system, that is, to appearance of the sharp $(\sqrt{3} \times \sqrt{3})$R30° LEED pattern at the first stage of reaction. Further low temperature chlorine dosing leads to the splitting of the overlayer spots into the six-spots triangles similar to the case of Cl/Cu(111),[8,16,18] I/Cu(111),[17] Br/Cu(111),[19] and I/Ag(111),[20] and, finally, the same "complex" diffraction pattern is observed. Heating of the sharp $(\sqrt{3} \times \sqrt{3})$R30° structure to 300 K gave rise to complete disappearance of the chlorine spots, while a heating of the system exhibiting the six-spot pattern resulted in a diffuse $(\sqrt{3} \times \sqrt{3})$R30° pattern.

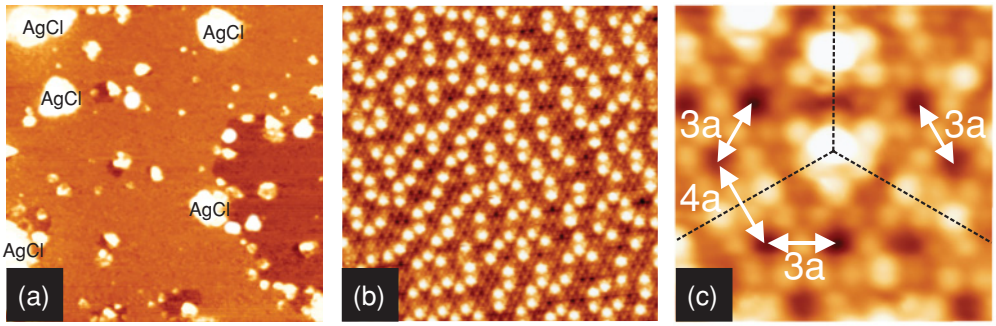

FIG. 1. (Color online) (a) Panoramic STM image (3000 × 3000 Å^2, $U_s = -8$ V, $I_t = 0.2$ nA, 5 K) of Ag(111) after adsorption of 5000 L of molecular chlorine at 300 K. (b) Typical STM image (292 × 292 Å^2, $U_s = -1$ V, $I_t = 1.6$ nA, 5 K) of saturated chlorine layer on the atomic terrace demonstrating coexistence of the bright objects and islands of the (3 × 3) reconstruction. (c) An atomic-resolution STM image (40 × 40 Å^2, $U_s = -1.4$ V, $I_t = 0.5$ nA, 5 K) showing atomic structure of bright clusters.

Recently we have shown that the application of low-temperature (5 K) scanning tunneling microscopy in a combination with DFT calculations makes possible recognition of atomic structures formed by chlorine on silver surface.[21] In particular, we have shown that complex pattern C observed by many authors is explained by the diffraction on a system of the antiphase (3 × 3) nanodomains formed in the course of the reconstruction of the upper silver layer.

In this work we have examined a saturated layer of chlorine formed on Ag(111) at room temperature. According to the notation made by Bowker *et al.*,[2] this coverage corresponds to a LEED pattern marked as D. Although, in the course of the C–D transformation the Cl/Ag AES peak ratio increases only by 15%,[2] the structure of the chlorinated surface may exhibit significant modifications. Indication on the surface restructuring at this coverage range can be found in the low energy ion scattering data published by Wu *et al.*[22] The authors observed that signal of chlorine increases with chlorine exposure reaching its maximum at the coverage slightly below the saturation level. Further increase of the coverage gives rise to the drop of chlorine signal down to zero level at saturation point.[22] Taking into account a high surface sensitivity of low energy ion scattering technique, one can suggest the formation of a new type of reconstruction with upper atomic layers mainly consisting of silver atoms.

The aim of the present paper is to recognize atomic structure of saturated chlorine coverage on Ag(111) using low temperature scanning tunneling microscopy in a combination with DFT calculations.

II. EXPERIMENTAL AND COMPUTATIONAL METHODS

All experiments were carried out in a UHV setup containing Omicron LT-STM operating at 5–77 K and LEED optics. The silver (111) sample was prepared by repetitive circles of Ar^+ bombardment (1 keV) and annealing up to 800 K. Chlorine inlet on Ag(111) surface was done at room temperature using a fine leak piezovalve.

All DFT calculations were carried out using the Vienna *ab initio* simulation package (VASP)[23–26] employing the projector augmented wave method[27] and PBE (Perdew, Burke, Ernzerhof) functional.[28] The plane-wave cut-off energy of 375 eV was applied. The silver substrate was modeled by a four layer slab. During structure optimizations the top layer of Ag atoms as well as the chlorine overlayer atoms were allowed to relax, while the bottom three layers of Ag were held fixed. A vacuum layer with a thickness of 14 Å was inserted between two neighboring slabs. The integration of Brillouin zone was done using Monkhorst-Pack[29] k-point mesh (14 × 14 × 1) per (1 × 1) of Ag(111). STM images were simulated from the DFT results using the simple Tersoff-Hamann approximation[30] considering states between E_F and $E_F - 0.5$ eV.

III. RESULTS AND DISCUSSION

Figure 1(a) shows a panoramic STM image of Ag(111) surface after exposure of 5000 L of molecular chlorine at 300 K. We associate a number of 3D objects with a height of 15–100 Å clearly seen in STM image with silver chloride islands.

We believe that atomic structure on the terraces which coexist with 3D silver chloride islands should correspond to a so called saturated chlorine layer.

The LEED pattern of such saturated layer did not exhibit appreciable changes in comparison with complex pattern C described in details in Ref. 21 with the exception of the little blurring of the spots and the growth of the background level associated with the appearance of the silver chloride islands.

According to the high-magnification STM image, the surface area between 3D islands is covered by array of the small bright objects. A typical STM image of a such coverage is shown in Fig. 1(b). According to the STM image, approximately one half of the surface is covered by domains with characteristic corner holes. This type of reconstruction of chlorinated Ag(111) surface has been considered in our recent paper[21] for the separate domains with the local (3 × 3) periodicity. The size of most domains with reconstruction is even less than a (3 × 3) unit cell, as seen from Figs. 1(b) and 1(c). For this reason, in further discussion we will call this reconstruction (3 × 3)-like.

The atomic-resolution STM image presented in Fig. 1(c) indicates that each bright object can be considered as a cluster with a six-atom basement and bright atom (or group of atoms) in the middle. Clusters play the role of domain boundaries between three adjacent antiphase domains of (3 × 3)-like reconstruction, as shown in Fig. 1(c).

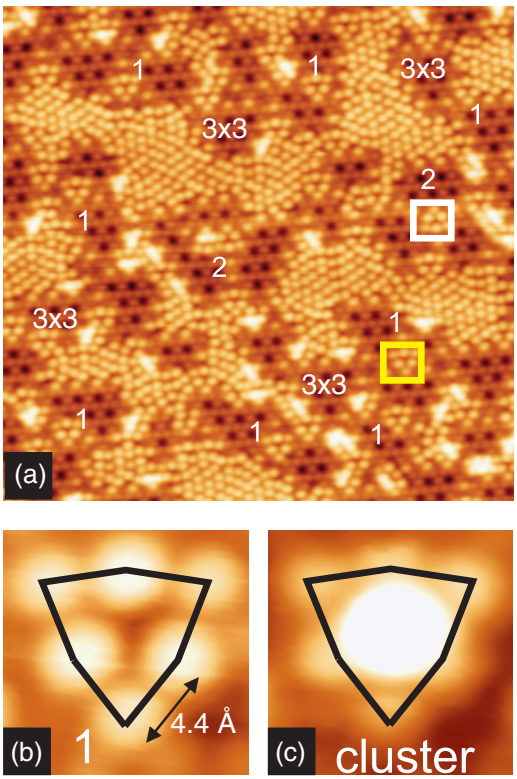

FIG. 2. (Color online) (a) STM image (206×200 Å^2, $U_s = -1.2$ V, $I_t = 1.6$ nA, 5 K) of chlorinated Ag(111) corresponded to LEED pattern C. Triangular domain boundaries with two possible orientation are indicated as 1 and 2. (b), (c) Fragments of the STM images of domain boundary between three (3 × 3) domains and cluster formed at "saturation."

To clarify the process of clusters formation, we looked again at the STM image of the chlorinated Ag(111) surface acquired at a lower coverage (see Fig. 2). At this stage of adsorption, separate domains of the (3 × 3)-like reconstruction coexist with disordered structure approximately corresponded to a compressed ($\sqrt{3} \times \sqrt{3}$)R30° lattice, as shown in Fig. 2. In our previous paper[21] we have concentrated on the atomic structure of the islands with the (3 × 3)-like reconstruction. Here we will focus on the atomic structure of boundaries between the adjacent (3 × 3) domains. According to Fig. 2, the most interesting objects are formed on the boundary between *three* adjacent (3 × 3) domains. They have a shape of triangles consisting of six chlorine atoms. The arrangement of atoms in the boundary and in the basement of the clusters appears to be exactly the same, as shown in Fig. 2(b). *Therefore we believe that clusters are formed on top of the domain boundaries between (3×3) domains.* In this connection, it is of great importance to understand the atomic structure of the domain boundary including the structure of the underlying silver layer.

Note also that atoms belonging to these six-atom triangles always look brighter in STM images than atoms belonging to the (3 × 3) domains. Moreover, they are looking exactly the same as atoms from a disordered compressed ($\sqrt{3} \times \sqrt{3}$)R30° lattice. In some places, one side of the triangle is even incorporated in the disordered layer (see Fig. 2).

Now we turn to the construction of the atomic scale model of the domain boundaries formed between (3 × 3) domains. Figure 3(a) shows an STM image obtained with high magnification of the three antiphase (3 × 3) domains and the six-atom boundary in the middle. We tried to reproduce all the features of the experimental image using the model of the (3 × 3)-like reconstruction proved in our recent paper.[21]

According to this model, within a (3 × 3) unit cell six Ag atoms in the top layer are arranged in two triangles with atoms occupying fcc and hcp sites, respectively. Chlorine atoms may be placed between four Ag atoms and in the off-center position in the hole.[21] Thus the building block of the silver layer reconstruction consists of three silver atoms. If we start to span the surface with such building blocks simultaneously for three antiphase domains giving positions of the corner holes from the experimental STM image, then we will see the formation of boundaries between domains. There are two types of the boundaries. First type arises along the line of contact of two domains. Due to the symmetry of the system one can find three equivalent directions of this type of boundaries shown in Fig. 3 by dashed line. On these lines new triangles consisting of six silver atoms are formed. It is worth noting that some atoms forming these triangles participate in the (3 × 3)-like reconstruction in *two adjacent domains*. Due to increase of the size of the silver triangle making domain boundaries there is an additional threefold adsorption site in the middle also occupied

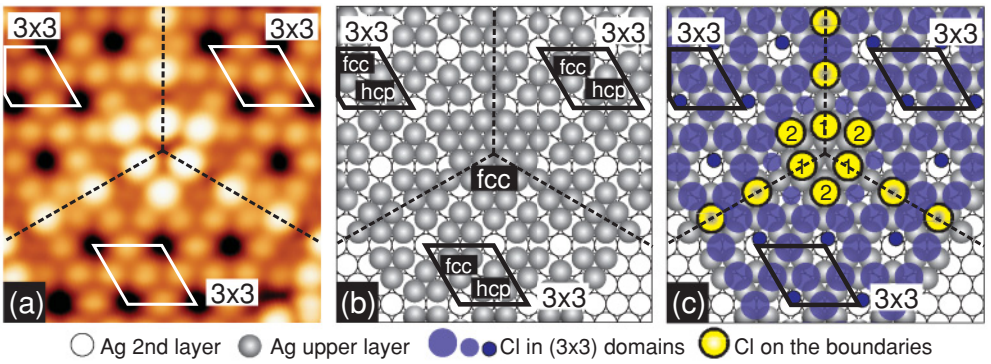

FIG. 3. (Color online) (a) The fragment of the experimental STM image (40×40 Å^2, $U_s = -1.2$ V, $I_t = 1.6$ nA, 5 K) of the boundary between three 3 × 3 islands. (b) Hard ball model demonstrating arrangement of silver atoms in the upper layer in each of three 3 × 3 domains and under the domain boundary. Formation of the big fcc triangle with 1×1 periodicity is clearly seen; (c) Hard ball model showing positions of chlorine atoms on the basement from (b).

by bright chlorine atom. The second type of the boundary arises in the place of the intersection of *three antiphase domains*. According to the drawing presented in Fig. 3(b), it also has a triangular shape and contains 21 silver atoms packed in the (1×1) lattice. Similar to the case of more simple boundaries, the corners of this big silver triangle participate as building blocks in the (3 × 3)-like reconstruction in the neighboring domains. The (1×1) arrangement of the inner atoms in the triangle is necessary to produce threefold adsorption sites for six "bright" atoms adsorbed on the boundary in accordance with experimental STM image in Fig. 3(a). In our model, six chlorine atoms occupy two different threefold positions marked in Fig. 3(c) as 1 and 2 and form a characteristic bright chlorine triangle. Such atom positions perfectly reproduce interatomic distances of 4.4 Å measured in the STM image between neighboring atoms on the sides of triangles. The difference in adsorption sites explains the different brightness of the three corner atoms and three side atoms.

As it follows from the STM image in Fig. 2, there are two different orientations of six-atom chlorine triangles on the surface ("corner up" and "corner down"). If we assume that silver atoms in the (1 × 1) triangle lying in the basement of the domain boundary in Fig. 3 occupy fcc positions, then silver atoms in the basement of the domain boundary with opposite orientation should occupy hcp sites.

To determine the atomic structure of clusters, we used DFT calculations with VASP code. In general case, clusters do not form a periodic lattice. However, in some places clusters form a new "rosette-like" superstructure described by a (7 × 7) unit cell as shown in Fig. 4(a). Taking into account that the basement of each cluster is formed by a triangle of 21 silver atoms with (1 × 1) periodicity (Fig. 3), we present in Fig. 4(b) a model showing arrangement of silver atoms in the basement of the (7 × 7) reconstruction. Within (7 × 7) unit cell there are two oppositely oriented triangles of silver atoms. In the first triangle, atoms occupy fcc sites, whereas in the second one hcp. Chlorine atoms may occupy threefold hollow adsorption sites on silver triangles marked as 1 and 2 forming a characteristic chlorine triangle, as shown in Figs. 4(c) and 4(d). Between silver triangles there are nearly fourfold hollow adsorption sites marked as 3 similar to the case of the original (3 × 3)-like reconstruction. Similar to the case of the (3 × 3)-like reconstruction, the holes in the corners of the (7 × 7) unit cell are occupied by chlorine atoms in positions 4.

Note that a complete (7 × 7) reconstruction is not realized in a real experiment even at saturation coverage. However, from the theoretical point of view it appears to be very convenient for DFT modeling of the clusters due to minimum size of the unit cell. That is why all model calculations performed for clusters were made using the (7 × 7) unit cell.

In our DFT calculations we considered all the stages of clusters formation. First, a simple model of the six chlorine atom triangle was considered [see Fig. 5(a)]. Using a Tersoff-Hammann approach,[30] we have calculated a theoretical STM image for this structure. The result of calculations obviously reproduces all features of the experimental STM image including a difference of the brightness between chlorine atoms in different types of the threefold positions [marked in Fig. 4(d) as 1 and 2].

On the next stage we have tested two simple structures with an additional chlorine or silver atom placed in the middle of a six-atoms chlorine triangle. The models and results of calculations are shown in Figs. 5(b) and 5(c) together with an experimental STM image of the cluster. We see that the

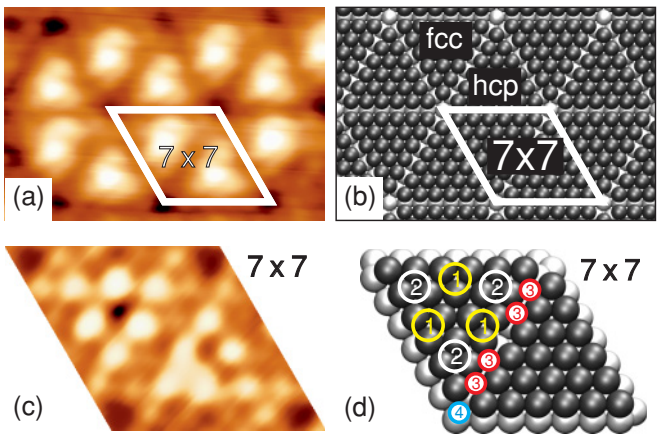

FIG. 4. (Color online) (a) The fragment of the experimental STM image (81 × 41 Å^2, $U_s = -0.8$ V, $I_t = 0.8$ nA, 5 K) demonstrating partial ordering of clusters in a (7 × 7) superstructure. (b) The arrangement of silver atoms in upper layer corresponded to the STM image from (a). (c) and (d) STM image ($U_s = -1.2$ V, $I_t = 1.6$ nA) and hard ball model of the (7 × 7) reconstruction. Different adsorption sites for chlorine atoms are indicated. Threefold positions marked as 1 and 2 correspond to atoms in the basement of clusters. Chlorine atoms also occupy the site 3 with nearly fourfold symmetry and the corner-hole site 4 as in original (3 × 3) reconstruction.

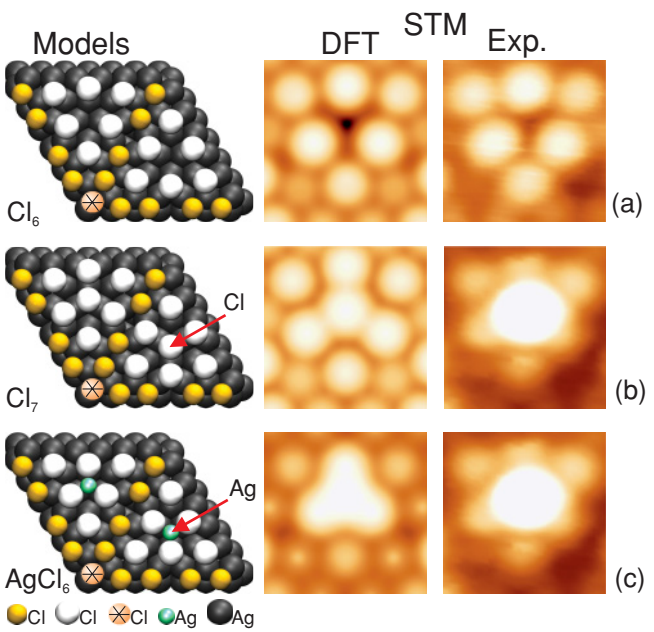

FIG. 5. (Color online) (a) Structural model of the initial chlorine six-atom triangle and corresponding theoretical STM image shown in comparison with experimental STM image. (b) and (c) Cluster models Cl_7 and $AgCl_6$ together with theoretical STM images shown in comparison with STM image of the cluster obtained at saturation of chlorine coverage.

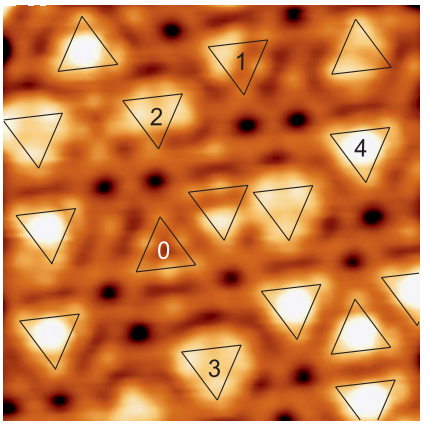

FIG. 6. (Color online) Experimental STM image (70×70 Å^2, I_t = 1.5 nA, U_s = +536 mV, 5 K) of the intermediate chlorine coverage on Ag(111) demonstrating different stages of clusters formation. 0 are unfilled initial triangles, 1 are one additional object in the corner, 2 are two objects in the corners, 3 are three objects in each corner, and 4 are a complete cluster.

correspondence of both theoretical images with the experiment is rather poor.

To look for a correct model, we considered an STM image corresponding to the case of incompletely formed clusters, as shown in Fig. 6. One can find five different types of objects on the surface. A simple triangle containing six chlorine atom is marked as 0. In all objects marked as 1 we detect a light spot in one of the corners of triangle. In the objects 2 already two corners are occupied, and in the objects 3 there is a light spot in each corner of triangle. Note also, the presence of the distinct minimum in the center of the object 3. Finally, we marked as 4 the complete clusters with characteristic bright spots in the center of triangle. We believe that objects 1–4 represent the stages of clusters formation. In this process the initial basement 0 accumulates step-by-step four additional atoms (chlorine and/or silver).

We also assume clusters to be AgCl particles of the minimum size taking into account their formation at saturated coverage. Indeed, the bulk crystal of silver chloride of NaCl type consists of two face cubic lattices of silver and chlorine, as seen from Fig. 7(a). Chlorides of fcc metals are known to grow on metal surfaces with their hexagonal plane being parallel to the substrate.[31–34] In Fig. 7(b) a perspective projection of the AgCl "cube" on a {111} plane is presented. We see that the

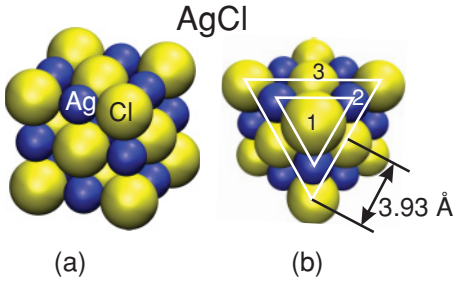

FIG. 7. (Color online) The crystal structure of AgCl (NaCl type). (a) 3D view. (b) Perspective projection of AgCl structure on the {111} plane. Three upper planes are indicated as 1, 2, and 3.

upper plane consists of a single chlorine atom from the corner of the cube. Next plane contains three silver atoms. Finally, in the third plane we see a triangle of six chlorine atoms, being similar to the triangle in the basement of the clusters in our experiments. Thus, by analogy with bulk silver chloride structure, we can assume that a model of silver chloride cluster Ag_3Cl_7 (Cl-Ag3-Cl6) is a natural choice for the explanation of our experimental data. Note also, that additional silver atoms necessary for Ag_3Cl_7 formation could come from the upper silver substrate layer in the course of the (3×3)-like reconstruction.

Figure 8 presents optimized models and corresponding theoretical and experimental STM images ($U_s = -500$ mV) describing the stages of Ag_3Cl_7 formation on the basement of a six-atom triangle. According to our calculations, an additional silver atom in a corner of the triangle gives rise to appearance of the light feature in a good correspondence with the experimental observation [Fig. 8(a)]. These kind of objects (cluster $AgCl_6$) appear in the STM images rather early simultaneously with islands of the (3×3)-like reconstruction, as seen from Fig. 2(a). Further DFT calculations were performed for cluster Ag_2Cl_6 corresponding to occupancy of two corners of triangles with silver atoms. Excellent agreement of theoretical STM image and experimental images is obvious

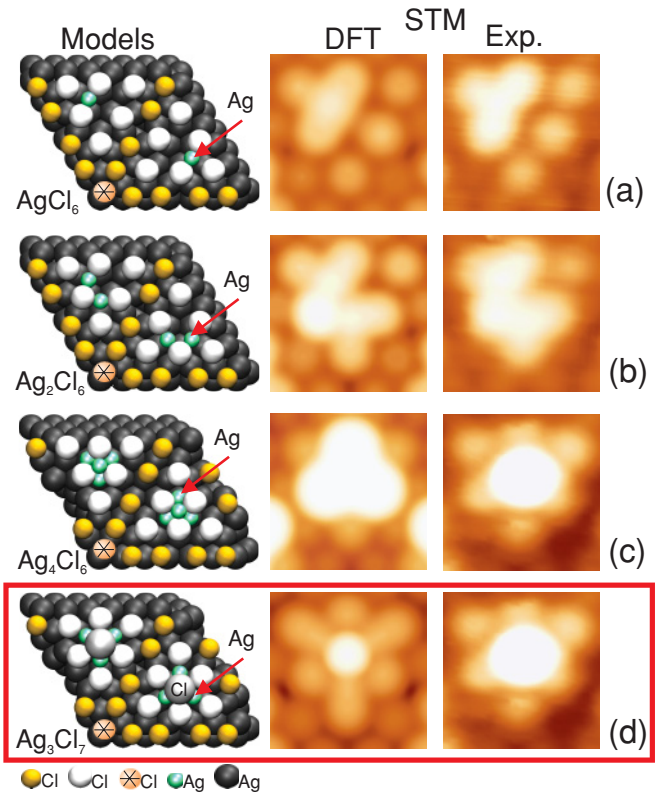

FIG. 8. (Color online) Structural models describing the formation of clusters and corresponding theoretical STM images shown in comparison with experimental observations. (a) Cluster $AgCl_6$, (b) Cluster Ag_2Cl_6, (c) Cluster Ag_4Cl_6, (d) Cluster Ag_3Cl_7. Theoretical STM images for (a) and (b) are shown in comparison with appropriate experimental STM frames acquired at intermediate coverages. For (c) and (d) comparison was made with STM image of cluster obtained at saturation.

from Fig. 8(b). A cluster Ag_3Cl_6 with three silver atoms in the corners of the triangle was also considered with DFT. However, it is not shown in Fig. 8, since we were not able to acquire a high-resolution STM image of such objects at negative bias voltage required for the correct comparison with the theoretical image. At positive voltages (see Fig. 6), the resolution appeared to be much worse.

On the final step of the cluster design we have tested silver [Fig. 8(c)] and chlorine atoms [Fig. 8(d)] placed above the center of Ag_3Cl_6 cluster. We see that the model with four silver atoms does not correspond to the experimental observation, whereas the theoretical STM image of the Ag_3Cl_7 pyramid with a chlorine atom on top and the experimental STM image of a cluster observed at saturation are very similar.

Thus, we have shown that a 2D array of clusters Ag_3Cl_7 is formed on the Ag(111) surface at saturation of chlorine coverage. The sequence of atomic layers in Ag_3Cl_7 corresponds well to the sequence of layers in a silver chloride bulk crystal in the direction ⟨111⟩. Optimized atomic coordinates for the Ag_3Cl_7 model obtained as a result of the DFT calculations are presented in Table I.

It is of interest to analyze the atomic structure of the Ag_3Cl_7 pyramid in comparison with AgCl lattice. In the case of bulk AgCl the interplane distances in a ⟨111⟩ direction are equal to 1.60 Å.[35] In the case of Ag_3Cl_7, the distance between upper chlorine atom and the plane consisting of three silver atoms is equal to 1.468 Å that roughly corresponds to a bulk value. In our model, pairs of atoms Ag1-Ag2, Ag2-Ag3, and Ag3-Ag1 are separated by distance of 3.636 Å that is slightly less than the nearest neighbor distances in a (111) plane of bulk AgCl crystal equaled to 3.93 Å.[35] Our calculations show that silver atoms (Ag1, Ag2, Ag3) occupy approximately threefold hollow adsorption sites above upper silver layer. The same threefold hollow positions are also occupied by six chlorine atoms from the basement of cluster. That is why the short distance (≈0.39 Å) between silver plane in Ag_3Cl_7 and an average basal chlorine plane is not surprising. Note, that we also obtained a little contraction of the nearest-neighbor chlorine distances in a basal chlorine plane (≈4.13 Å) in comparison with Cl-Cl distances in a six-atom domain boundary from Fig. 2(b) (≈4.4 Å).

Thus, according to our analysis, the upper chlorine atom and three silver atoms occupy positions in a slightly distorted AgCl lattice. The basement of the Ag_3Cl_7 cluster could be considered in some sense as an interface between Ag(111) substrate and cluster Ag_3Cl.

TABLE I. Atomic coordinates of chlorine and silver atoms in the Ag_3Cl_7 cluster.

Atom label	x_{DFT} (Å)	y_{DFT} (Å)	z_{DFT} (Å)[1]
Cl0	0.000	11.928	11.218
Ag1	−1.818	12.978	9.752
Ag2	1.818	12.978	9.752
Ag3	0.000	9.829	9.752
Cl1	−4.023	14.251	9.393
Cl2	0.000	15.198	9.334
Cl3	4.023	14.251	9.393
Cl4	2.832	10.293	9.334
Cl5	0.000	7.283	9.393
Cl6	−2.832	10.293	9.334

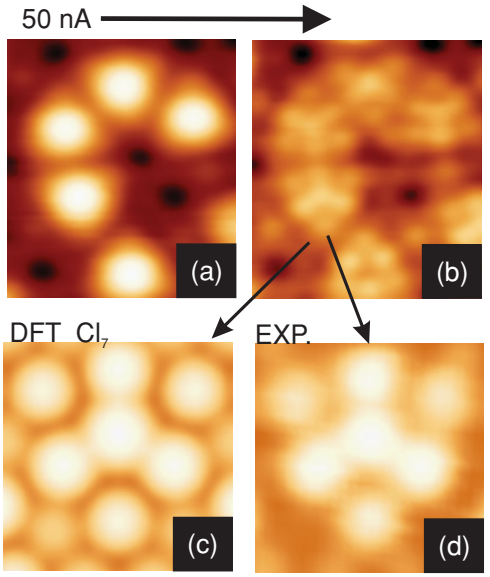

FIG. 9. (Color online) STM images (36×40 Å^2, I_t = 1.5 nA, U_s = +536 mV, 5 K) (a) before and (b) after the scanning of the current frame with tunnel current 50 nA. (c) Theoretical image of Cl_7 cluster, (d) High resolution STM image (I_t = 1.5 nA, U_s = −500 mV) of the cluster modified by the tip action.

It is noteworthy that Ag_3Cl_7 clusters are rather soft and can be easily modified by the tip of STM even at 5 K. Indeed, we found out that raising the tunnel current to 50 nA leads to the modification of clusters, as shown in Figs. 9(a) and 9(b). We see that all the bright objects were removed from the basement. Even after action of the tip the centers of some triangles remain to be occupied. The high-resolution STM image of this new object shown in Fig. 9(d) appears to be exactly the same as the theoretical STM image of the cluster Cl_7 initially presented in Fig. 6. Artificial cluster Cl_7 was never observed after room temperature chlorine adsorption. In any case, this observation is an additional support of the structural model suggested for the description of experimentally observed clusters.

IV. CONCLUSIONS

In conclusion, using LT-STM and DFT we have determined the morphology and the atomic structure of the saturated chlorine coverage on Ag(111) formed as a result of the room temperature adsorption. According to our findings, two different phases coexist on the surface: islands with a (3 × 3)-like reconstruction and clusters Ag_3Cl_7. The process of the final structure formation is self-consistent. In other words, silver atoms extracted from the substrate in the process of the (3 × 3)-like reconstruction participate in formation of clusters on the boundaries between adjacent (3 × 3) domains. We have discovered a new type of the surface object (cluster Ag_3Cl_7) never discussed previously in the literature for Cl/Ag system.

We think that Ag_3Cl_7 clusters hardly can be considered as nuclei for the growth of 3D silver chloride islands. To build 3D silver chloride crystallite one should have a source of silver atoms. On the atomic terraces such a source has a

limited capacity determined by the number of atoms extracted in the course of the (3×3) reconstruction. In other words, the number of available silver atoms on the terrace is not enough to build multilayer chloride. Moreover, when the saturated layer (3×3 and Ag_3Cl_7) forms, it becomes very difficult to extract additional silver atoms. That is why the sticking probability of chlorine drastically decreases after formation of saturated layer.[2] The preferable growth of 3D silver chloride starts on the step edges, the natural defects of the surface. We believe that at such places it is easier to extract silver atoms necessary for the AgCl lattice construction. From our data we cannot definitely say that saturated layer remains under the AgCl islands. However, our recent data for the AgI film growth on Ag(100) indicate that saturated monolayer remains as an interface between substrate and halide film.[34]

Our result could be interesting in the explanation of the thermodesorption spectra obtained in the work of Bowker *et al.*[2] Here we evidently demonstrated the presence of two different phases on the surface at saturation. It is likely that clusters contribute to the "multilayer peak," while chlorine from domains with a (3×3)-like reconstruction desorbs in the "monolayer peak." The energy of desorption for both phases could be quite similar, which explains intersection of the thermodesorption peaks.

On the basis of our results it becomes possible to recognize the unusual behavior of the chlorine signal in low energy ion scattering experiments published by Wu *et al.*[22] In our interpretation, after formation of the clusters the main part of chlorine atoms becomes screened by the upper silver atoms belonging to the clusters. Another point concerned the promotional effect of chlorine in a reaction of ethylene epoxidation. According to Campbell[36] the selectivity of the reaction increases with chlorine coverage, however speed of reaction goes to zero at saturation of chlorine coverage. In our work, at coverage slightly below the saturation we observed uncomplete clusters Ag_3Cl_6, Ag_2Cl_6, and $AgCl_6$. The chemical state of the silver atoms in these structures could be different from that of atoms from the bulk. Therefore, the system can be interesting from the point of view of oxygen adsorption into these new adsorption sites that could be important in the further studies of mechanism of epoxidation reaction.

ACKNOWLEDGMENTS

This work was supported in part by grants of the Russian Foundation for Basic Research No.10-02-90476-Ukr-a, by Contracts No. P2452, No. P2293, and No. P177 with Russian Federal Agency for Education. We thank Chair of Informatics, Moscow Institute of Physics and Technology, for making their MIPT-60 high performance computing system available for this work.

*andrush@kapella.gpi.ru

[1] J. G. Serafin, A. C. Liu, and S. R. Seyedmonir, J. Mol. Catal. A **131**, 157 (1998).
[2] M. Bowker and K. C. Waugh, Surf. Sci. **134**, 639 (1983).
[3] M. Bowker and K. C. Waugh, Surf. Sci. **155**, 1 (1985).
[4] M. Bowker and K. C. Waugh, Surf. Sci. **179**, 254 (1987).
[5] B. V. Andryushechkin, K. N. Eltsov, V. M. Shevlyuga, and V. Y. Yurov, Surf. Sci. **431**, 96 (1999).
[6] G. Rovida, F. Pratesi, M. Maglietta, and E. Ferroni, Japan J. Appl. Phys. Suppl. **2**, 117 (1974).
[7] G. Rovida and F. Pratesi, Surf. Sci. **51**, 270 (1975).
[8] P. J. Goddard and R. M. Lambert, Surf. Sci. **67**, 180 (1977).
[9] Y. Y. Tu and J. M. Blakely, J. Vac. Sci. Technol. **15**, 563 (1978).
[10] K. Wu, D. Wang, J. Deng, X. Wei, Y. Cao, M. Zei, R. Zhai, and X. Guo, Surf. Sci. **264**, 249 (1992).
[11] G. M. Lamble, R. S. Brooks, S. Ferrer, D. A. King, and D. Norman, Phys. Rev. B **34**, 2975 (1986).
[12] B. V. Andryushechkin, K. N. Eltsov, V. M. Shevlyuga, and V. Y. Yurov, Surf. Sci. **407**, L633 (1998).
[13] R. G. Jones, Prog. Surf. Sci. **27**, 25 (1988).
[14] E. I. Altman, in *Physics of Covered Solid Surfaces: Part I. Adsorbed Layers on Surfaces*, edited by H. P. Bonzel (Springer, Berlin, 2001), pp. 421–453.
[15] A. G. Shard and V. R. Dhanak, J. Phys. Chem. B **104**, 2743 (2000).
[16] B. V. Andryushechkin, K. N. Eltsov, and V. M. Shevlyuga, Surf. Sci. **470**, L63 (2000).
[17] B. V. Andryushechkin, K. N. Eltsov, and V. M. Shevlyuga, Surf. Sci. **472**, 80 (2001).
[18] W. K. Walter, D. E. Manolopoulos, and R. G. Jones, Surf. Sci. **348**, 115 (1996).
[19] M. Kadodwala and R. G. Jones, Surf. Sci. **370**, L219 (1997).
[20] U. Bardi and G. Rovida, Surface Science **128**, 145 (1983).
[21] B. V. Andryushechkin, V. V. Cherkez, E. V. Gladchenko, G. M. Zhidomirov, B. Kierren, Y. Fagot-Revurat, D. Malterre, and K. N. Eltsov, Phys. Rev. B **81**, 205434 (2010).
[22] K. Wu, D. Wang, X. Wei, Y. Cao, and X. Guo, Surface Science Letters **285**, L522 (1993).
[23] G. Kresse and J. Hafner, Phys. Rev. B **47**, 558 (1993).
[24] G. Kresse and J. Hafner, Phys. Rev. B **49**, 14251 (1994).
[25] G. Kresse and J. Furthmuller, Comput. Mater. Sci. **6**, 15 (1996).
[26] G. Kresse and J. Furthmuller, Phys. Rev. B **54**, 11169 (1996).
[27] G. Kresse and D. Joubert, Phys. Rev. B **59**, 1758 (1999).
[28] J. P. Perdew, K. Burke, and M. Ernzerhof, Phys. Rev. Lett. **77**, 3865 (1996).
[29] H. J. Monkhorst and J. D. Pack, Phys. Rev. B **13**, 5188 (1976).
[30] J. Tersoff and D. R. Hamann, Phys. Rev. B **31**, 805 (1985).
[31] M. Galeotti, B. Cortigiani, M. Torrini, U. Bardi, B. Andryushechkin, A. Klimov, and K. Eltsov, Surf. Sci. **349**, L164 (1996).
[32] B. V. Andryushechkin, K. N. Eltsov, V. M. Shevlyuga, C. Tarducci, B. Cortigiani, U. Bardi, and A. Atrei, Surf. Sci. **421**, 27 (1999)
[33] B. V. Andryushechkin, K. N. Eltsov, and V. M. Shevlyuga, Surf. Sci. **566**, 203 (2004).
[34] B. V. Andryushechkin, G. M. Zhidomirov, K. N. Eltsov, Y. V. Hladchanka, and A. A. Korlyukov, Phys. Rev. B **80**, 125409 (2009).
[35] R. W. G. Wyckoff, *Crystal Structures* (Wiley, New York, 1963), Vol. 1.
[36] C. T. Campbell, J. Catal. **99**, 28 (1986).